The Journal of Neuroscience, August 1, 1998, *18*(15):5817–5831

Presynaptic Function during Muscle Remodeling in Insect Metamorphosis

Christos Consoulas and Richard B. Levine

Division of Neurobiology, University of Arizona, Tucson, Arizona 85721

During metamorphosis the leg neuromuscular system of the moth *Manduca sexta* undergoes an extensive remodeling as the larval muscles degenerate and are replaced by new muscles in the adult. The terminal processes of persistent leg motoneurons undergo severe regression followed by regrowth (Consoulas et al., 1996), accompanied, as shown here, by the loss and re-establishment of functional presynaptic specializations. Before and shortly after the degeneration of the larval muscle, immunoreactivity for the vesicular protein synaptotagmin was localized to the presynaptic varicosities of the motoneurons. Similarly localized were distinct sites of Ca^{2+}-dependent uptake of the fluorescent dye FM1-43. During myoblast migration and accumulation about the re-expanding motor axons, synaptotagmin immunoreactivity was widely distributed in axons, and specific FM1-43 staining revealed vesicle exocytosis in distal axon branches. During myoblast proliferation and fusion, and myotube formation, synaptotagmin staining remained widely distributed in nerve branches, whereas FM1-43 staining was more localized to subdomains of these nerve branches. These initial presynaptic active sites were transient and were replaced by new sites in more distal nerve processes as the muscle anlage increased in size and additional myotubes formed. After myotube separation, synaptotagmin staining disappeared from primary branches but remained distributed within secondary and high-order nerve branches. FM1-43 staining was detected in high-order branches only. During muscle fiber striation, growth, and maturation, both FM1-43 staining and synaptotagmin immunoreactivity became localized to terminal varicosities. Thus, presynaptic function can persist after the loss of the target and occurs transiently in axon shafts before becoming restricted to terminal domains as the underlying muscle fibers mature.

Key words: insect; neuromuscular junctions; motor terminals; presynaptic; FM1-43; synaptotagmin

Functional signal transmission at the neuromuscular junction requires the precise alignment and differentiation of specialized regions of both the presynaptic and postsynaptic cells. This alignment is maintained in the mature organism through cell contact and diffusible signals between nerve and muscle (Hall and Sanes, 1993; Connor and Smith, 1994; Keshishian et al., 1996). Postsynaptic receptors that are initially diffusely distributed on the myotube surface become localized to the postsynaptic region because of signals from the motoneuron (Broadie and Bate, 1993a,b; Hall and Sanes, 1993). Similarly, the alignment of presynaptic active sites and the clustering of synaptic vesicles at those sites depend on signals derived from the muscle (Sanes et al., 1978; Hall and Sanes, 1993; Noakes et al., 1995).

Although the synthesis and distribution of synaptic vesicle proteins in growing neurites occurs before synaptic contact, the restriction to the presynaptic terminals is initiated after the initial growth cone–muscle fiber contact (Lupa and Hall, 1989; Littleton et al., 1993). Genetic elimination of target muscles in *Drosophila* does not prevent the formation of presynaptic zones, suggesting that their initial assembly is a process autonomous to the motoneurons, but correct localization is target-dependent (Prokop et al., 1996). Similarly, synaptic vesicles present in the axons of cultured hippocampal neurons can aggregate and undergo Ca^{2+}-dependent exocytosis in the absence of postsynaptic contacts (Kraszewski et al., 1995). Whether the aggregation of synaptic vesicles and their capacity for exocytosis in immature axons has a functional significance *in vivo* is not known. Similarly unclear are the mechanisms that ensure precise localization of presynaptic specializations once contact with an appropriate target is achieved or that allow this localization to be modified during postembryonic synaptic plasticity.

The leg neuromuscular system of the moth *Manduca sexta* undergoes a dramatic remodeling during metamorphosis that provides a useful model system for addressing the localization of presynaptic specializations. The larval legs and associated muscles degenerate and are replaced by a new set of legs and muscles in the adult (Kent et al., 1995; Consoulas et al., 1997). Both sets of muscles are innervated by the same population of motoneurons (Kent and Levine, 1988). The axons and terminal processes of these motoneurons remain in the periphery throughout metamorphosis but undergo extensive regression and growth (Consoulas et al., 1996). In the present study the functional remodeling of presynaptic motor terminals was investigated by following the redistribution of synaptotagmin, an integral membrane protein known to play a role in docking and fusion of synaptic vesicles (Perin et al., 1990), and the capacity for Ca^{2+}-dependent synaptic vesicle recycling, as assessed with the fluorescent dye FM1-43 (Betz and Bewick, 1992). Ca^{2+}-dependent vesicle exocytosis continues within regressed axons after muscle degeneration in the absence of a target during the early stages of motor terminal remodeling. As muscle fibers mature, sites of vesicular recycling shift within growing axons, progressively becoming restricted to

Received March 6, 1998; revised April 30, 1998; accepted May 21, 1998.

This work was supported by Grant NS 24822 from the National Institutes of Health. C.C. was supported by Fogarty International Center Fellowship TWO 4898. We thank Maria Anezaki for assistance with histology. We also thank Dr. Mani Ramaswami for introducing us to the FM1-43 labeling technique.

Correspondence should be addressed to Dr. Christos Consoulas, Division of Neurobiology, Room 611, Gould Simpson Building, University of Arizona, Tucson, AZ 85721.

mature presynaptic terminals. This remarkable example of synaptic remodeling provides a natural model for further exploration of cellular interactions that ensure proper neuromuscular function.

MATERIALS AND METHODS

Animals. M. sexta (L.) were obtained from a laboratory culture reared on an artificial diet (Bell and Joachim, 1976) under a long-day photoperiod regimen (17/7 hr light/dark cycle) at 26°C and ~60% relative humidity. Both chronological and morphological criteria were used for the staging of animals (Nijhout and Williams, 1974; Bell and Joachim, 1976; Reinecke et al., 1980; Tolbert et al., 1983; Consoulas et al., 1996, 1997). In summary, L0, L1, L2, and L3 represent the days of the last (fifth) larval instar, W0 signifies the first day of wandering, and W1 to W4 represent the remaining days before pupation. After pupation, stage P0 indicates the day of the pupal molt, and P1 through P18 are the next stages of adult development.

Nerve staining techniques. Biocytin filling was used to reveal the details of the peripheral branching of leg motoneurons (Horikawa and Armstrong, 1988; Consoulas et al., 1996). To fill the peripheral axons of the leg motoneurons in the orthograde direction, the animals were first anesthetized by chilling on ice. After removing the head and abdomen, the thoracic segments were dissected along the dorsal midline and pinned down on a Sylgard-coated Petri dish in saline. The whole prothoracic ganglion with intact nerves was isolated in a Vaseline pool to allow the infusion of a biocytin solution (3% w/v biocytin in distilled water; Sigma, St. Louis, MO). The preparations were stored at 7°C. After biocytin infusion for a maximum of 2 d, the preparations were dissected and fixed in freshly prepared solution containing 4% paraformaldehyde, 0.15% glutaraldehyde, and 0.2% saturated picric acid in 0.1 M phosphate buffer, pH 7.4, overnight (Sun et al., 1993). They were subsequently dehydrated in ethanol, permeabilized in xylol or propylene, rehydrated in ethanol, and washed in 10 mM PBS, pH 7.4, three times for 15 min each and in PBS containing 1% Triton X-100 (PBSX) three times for 15 min each. To block nonspecific staining the preparations were incubated in 10% normal goat serum (NGS; Jackson ImmunoResearch, West Grove, PA) and 3% bovine serum albumin (BSA; Boehringer Mannheim, Indianapolis, IN) in PBSX for 1 hr. They were then incubated in Cy3-conjugated streptavidin (Jackson ImmunoResearch) for 5–12 hr in 7°C. The preparations then were washed several times with PBS, dehydrated in ethanol, and cleared in methyl salicylate.

Synaptotagmin immunostaining. The distribution of immunoreactivity for the presynaptic protein synaptotagmin was examined in whole-mount preparations with a polyclonal antibody raised against *Drosophila* synaptotagmin (DSYT2; Littleton et al., 1993; generously provided by H. J. Bellen, Howard Hughes Medical Institute, Baylor University, Houston, TX). The protocol was similar to that used in a previous study of the *Manduca* leg system (Consoulas et al., 1996). Developing and adult leg muscles were dissected in cold saline and fixed in freshly made 4% paraformaldehyde for 1 hr at room temperature. After rinsing in 10 mM PBS and 10 mM PBS with 0.2% Triton X-100 (PBSX) for 2 hr, they were blocked for 1 hr (six times for 10 min each) in a Tris-HCl buffer, pH 7.0, containing 10% Triton X-100, 1% Na azide, 0.25% BSA, and 2% NGS. The preparations were then incubated overnight in primary antiserum (1:1000) made up in the blocking buffer. After washing in PBSX and PBS for 2 hr they were incubated in Cy3-conjugated secondary antibody for 4–8 hr at 4°C. The preparations were then rinsed in PBSX and PBS, dehydrated, and cleared in methyl salicylate. The results presented here are based on a minimum of 10 preparations from each developmental stage. No staining was observed at any developmental stage in parallel preparations in which no primary antibody was used. We have repeated with identical results the immunostaining of stages L2, P18, and critical intermediate stages (P4–P10) using a polyclonal antibody recently generated against *Manduca* synaptotagmin (kindly provided by S. H. Dubuque and L. P. Tolbert, Division of Neurobiology, University of Arizona, Tucson, AZ). The synaptotagmin protein shows a high degree of homology between the two insect species (Dubuque et al., 1997).

Preparations from different developmental stages were processed together in the same dish and viewed with a confocal microscope (see below). Background staining varied from stage to stage because of changes in the types of surrounding tissues (e.g., intact muscle, developing muscle, and epidermis). The background level on a gray scale was held constant among preparations to adjust for this variability. Thus, the aperture and neutral-density settings remained constant, whereas the gain and black-level settings were adjusted over a small range (1/10 of the full scale). These minor changes in microscope settings did not alter the apparent distribution of immunoreactivity as tested by varying the settings over this range while acquiring images of mature and developing stages.

Table 1. Working protocol for FM1-43 staining

Stage	n	Stimulation protocol	Washing time (min)
L2	9	5Hz, 5 min	20
W4	7	5Hz, 5 min	30 ± 5
P1, P2	11	5Hz, 5 min,or1Hz,10min[a]	60 ± 10
P4	13	1Hz,10min[a]	50 ± 15
P8	12	1Hz,10min[a]	50 ± 15
P10	10	5Hz, 5 min	40 ± 5
P14	5	5Hz, 5 min	20
P18	5	5Hz, 5 min	20

[a]The main nerve 2a was stimulated with pulses of 1 Hz for 5–20 sec with 30 sec intervals between trains. The total period of stimulation was 10 min.

FM1-43 staining. The fluorescent dye FM1-43 (Molecular Probes, Eugene, OR) was used to monitor synaptic vesicle exocytosis and recycling (Betz and Bewick, 1992). The legs were dissected from the animal and pinned to a Sylgard-coated Petri dish that was attached firmly with wax to a microscope slide. The leg nerve 2a was stimulated with a Grass Instruments S 88 stimulator via a saline-filled suction electrode with 1–5 Hz pulses for 5–10 min in the presence of 4 μM FM1-43 in saline (see Table 1 for specific details). The strength of stimulation was adjusted to recruit all of the pretarsal flexor motoneurons (see below). The saline consisted of (in mM): 140 NaCl, 5 KCl, 4 $CaCl_2$, 28 glucose, and 5 *N*-2-hydroxyethylpiperzeine-*N*′-ethanesulfonic acid, pH 7.4 (Trimmer and Weeks, 1989). The evoked postsynaptic responses were intracellularly recorded via glass electrodes filled with 2 M potassium acetate (tip resistance, 40–60 MΩ). The signals were amplified with an Axoclamp-2A (Axon Instruments) amplifier and recorded on an eight-channel video recording system (Vetter 3000A) and subsequently transferred to a computer (acquisition sample rate, 10 Khz) for analysis using Data-Pac II software (Run Technologies).

For imaging, preparations were transferred to a Bio-Rad (Cambridge, MA) 600 krypton/argon confocal laser scanning microscope and viewed through a Zeiss 40× water immersion objective (488 nm excitation filter). The same area could be viewed repeatedly, after FM1-43 unloading, reloading, and synaptotagmin staining, by aligning the slide at the same *x,y* coordinates on the microscope stage, in addition to using landmarks such as trachea. The specific pattern of staining that was observed was consistent with previous observations of insect neuromuscular junctions (Ramaswami et al., 1994). Experiments that were performed to ensure the specificity of staining are described in Results.

Muscle-staining techniques. In many cases the state of internal structures within the legs was examined in serial longitudinal sections. The legs were removed from the animals, fixed in alcoholic Bouin's fixative for 2–3 d, embedded in paraffin (paraplast), and serially sectioned (10–12 μm). After deparaffinization and rehydration, the sections were stained with hematoxylin-eosin.

5-Bromodeoxyuridine labeling. To reveal the number and locations of nuclei undergoing DNA replication cells, 50 μg/gm body weight 5-bromodeoxyuridine (BrdU, Sigma) dissolved in distilled water was injected into the animals at specific developmental stages 12 hr before their dissection. The prothoracic legs then were fixed for 2 d in alcoholic Bouin's or Carnoy's fixative, embedded in paraffin, and sectioned. After deparaffinization, rehydration, and extensive washing in PBS and PBSX (0.1% Triton X-100), the DNA was denatured by treatment with 2N HCl in PBS for 15 min. Nonspecific activity was blocked with 10% NGS in PBS for 30 min. The sections were then incubated for 2 hr in the primary antibody against BrdU (Becton Dickinson, Mountain View, CA) diluted 1:100 in PBS with 5% NGS. After washing the sections in PBSX and PBS for 1 hr, they were incubated in goat anti-mouse secondary antibody diluted 1:200 (Cy3- or fluorescein-conjugated, Sigma) in PBS for 1 hr.

Terminal deoxynucleotidyl transferase-mediated dUTP nick end label staining. Apoptotic nuclei of degenerating muscles were revealed with the terminal deoxynucleotidyl transferase-mediated dUTP nick end-labeling (TUNEL) technique following the instructions of the manufacturer (Boehringer-Mannheim).

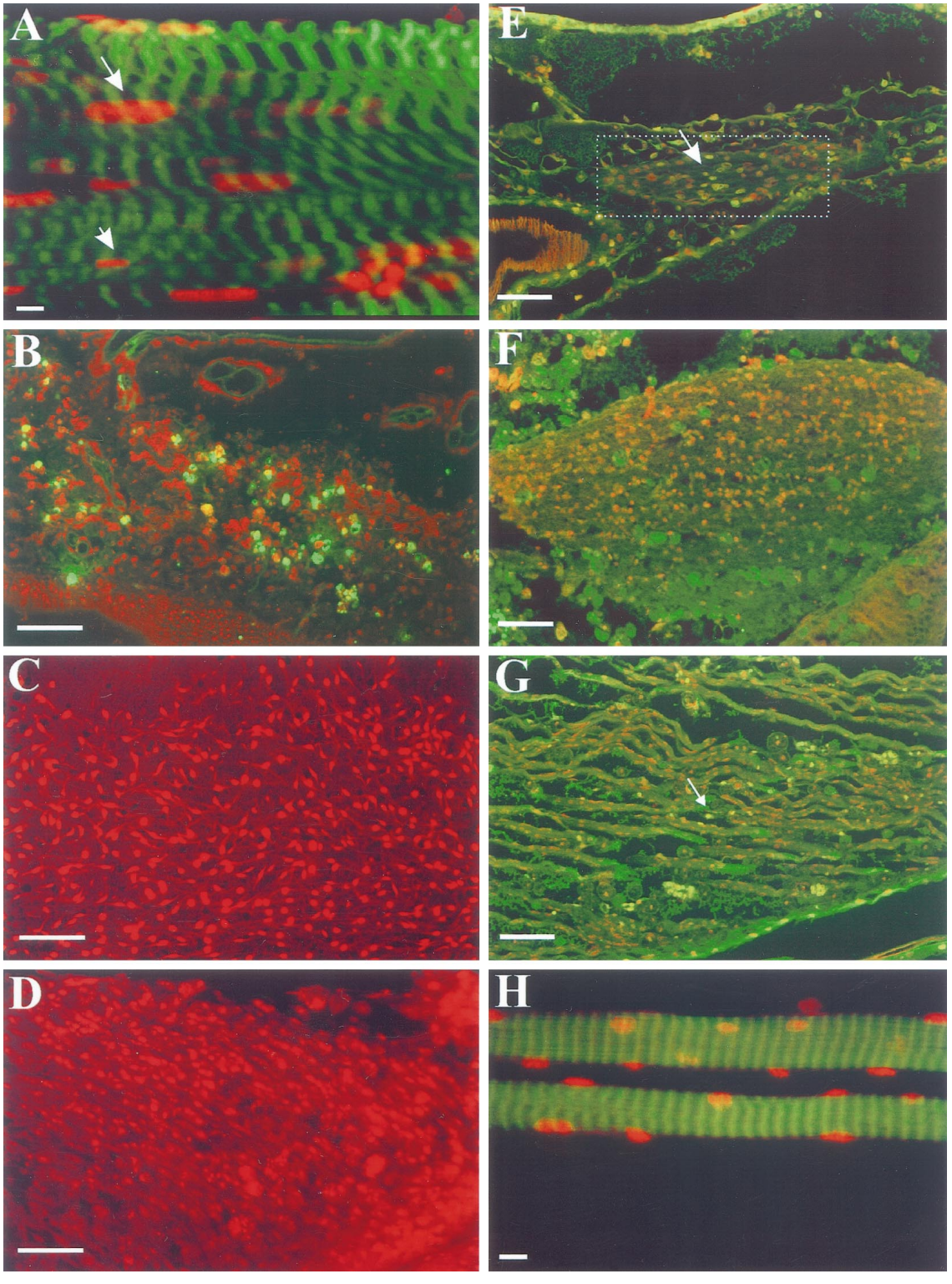

Figure 1. Remodeling of the PrtFlx muscle during metamorphosis. *A*, The larval (L2) PrtFlx muscle fibers are packed tightly together and bear nuclei of different sizes (*arrow*, large nucleus; *arrowhead*, small nucleus). Filamentous actin was revealed with Oregon Green phalloidin (*green*), and the myonuclei were stained with propidium iodide (*red*). *B*, Longitudinal section from a stage W2b-late leg processed by the TUNEL staining method (*green*) and counterstained with propidium iodide (*red*). The muscle fibers have broken down, and many of the myonuclei are apoptotic. *C*, Longitudinal section from the proximal femur of a stage P1 leg stained with propidium iodide. Myoblasts (mononucleate bipolar cells) are widely distributed within the imaginal leg during the early stages after pupation. *D*, By stage P3, myoblasts (propidium iodide staining) are aligning and beginning to fuse. *E–G*, Longitudinal sections of the PrtFlx muscle anlage. The nuclei undergoing DNA synthesis were labeled with an antibody against BrdU (*yellow* as a result to the colabeling with propidium iodide in *E*, *G*; *red* in *F*). Proliferation of myonuclei began by stage P3 (*E*) in a central area within the anlage (*arrow*) continued at a high rate at the time of myotube formation (stage P6, *F*) and decreased considerably by stage P8 (*G*, *arrow* indicates a nucleus that incorporated BrdU). *H*, The mature muscle fibers (stage P18), stained with Oregon Green phalloidin, are well separated from each other. The uniformly sized myonuclei, stained with propidium iodide (*red*), are distributed at the outer surface of the fibers. Scale bars: *A*, 20 μm; *B–G*, 100 μm; *H*, 20 μm.

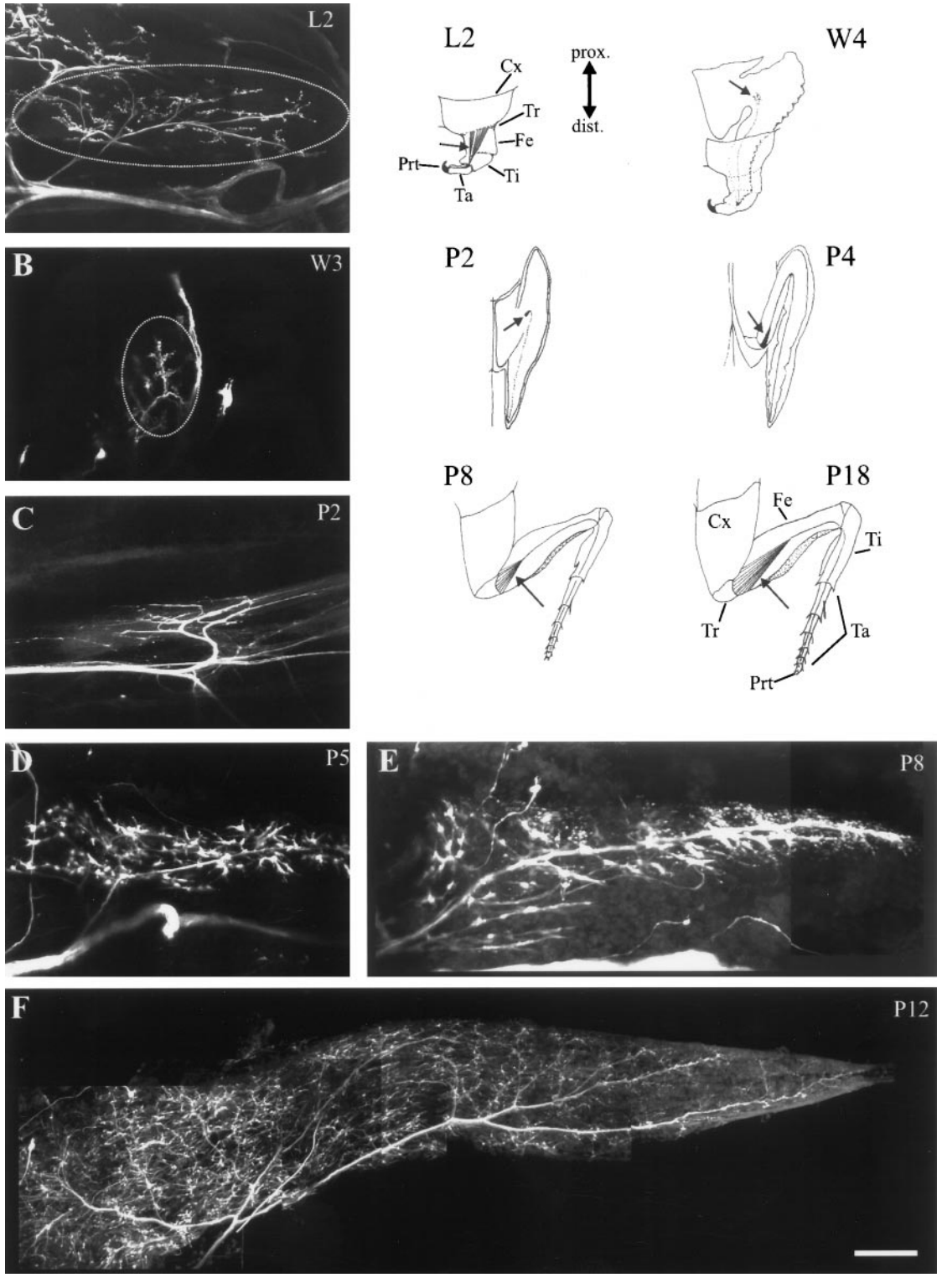

Figure 2. Remodeling of PrtFlx muscle innervation. Confocal micrographs were taken from whole-mount preparations in which the leg nerve 2a was filled with biocytin, and the staining was revealed with Cy3-conjugated streptavidin. *A*, Stage L2; PrtFlx motor axons branch extensively over the intact muscle (the innervation of one muscle bundle is shown, see *ellipse*). *B*, Stage W3; the complete degeneration of the muscle is accompanied by an extensive loss of high-order branches and terminal varicosities (*ellipse*). *C*, Stage P2; long motor axon processes grow over the imaginal epidermis. At the same time myoblasts begin to accumulate close to the nerve branches. *D–F*. Stages P5, P8, P12; extensive growth of the nerve branches occurs within the borders of the developing muscle anlage. Thin terminal processes emerging from high-order branches are apparent. At the same time myonuclei proliferate and muscle fibers form. The elongation of the muscle fibers and the adult pattern of nerve branching have been completed by stage P12. Each fiber is supplied by high-order nerve branches. During subsequent days of muscle development, presynaptic varicosities differentiate over the muscle fibers (see Figs. 3, 4). Stages are indicated at the *top right* of each panel. Scale bar, 0.1 mm. The camera lucida drawings in *insets* describe the formation of the adult leg and the position of the PrtFlx muscle or muscle anlage (*arrows*). The drawings are not to scale. *Cx*, Coxa; *Fe*, femur; *Prt*, pretarsus; *Ta*, tarsus; *Ti*, tibia; *Tr*, trochanter.

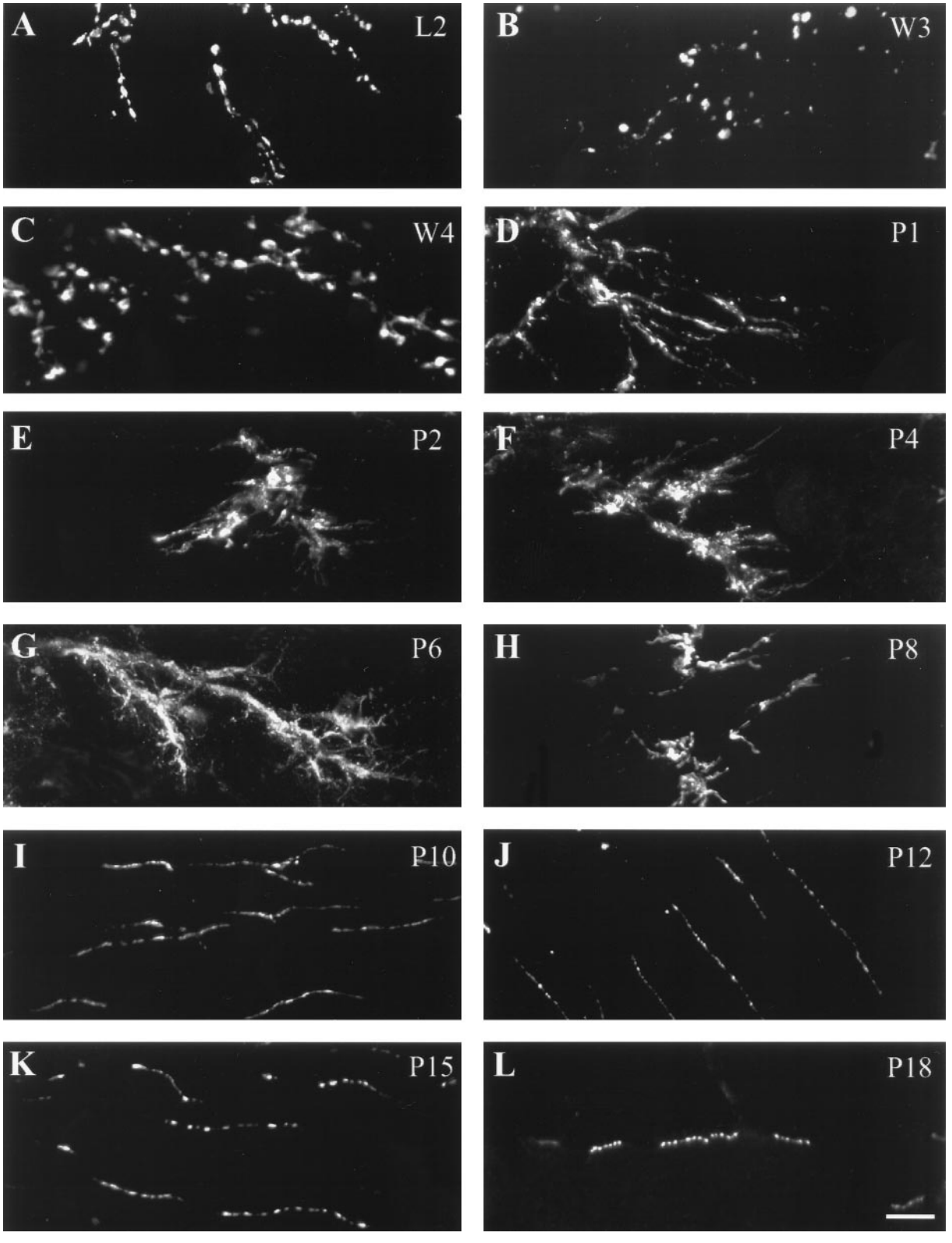

Figure 3. Confocal micrographs taken from whole-mount preparations that were stained with a polyclonal synaptotagmin antibody (anti-DYST2). Developmental stages are indicated at the *top right* of each panel. *A*, The larval PrtFlx muscle is intact. Synaptotagmin immunoreactivity is localized in presynaptic varicosities. *B, C*, PrtFlx muscle is degenerating. Synaptotagmin immunoreactivity remains localized in enlarged terminal varicosities despite the absence of the target muscle. *D–G*, Early stages of adult PrtFlx muscle formation. Synaptotagmin immunoreactivity is distributed in a punctate manner within the primary, secondary, and high-order motor axon branches. *H*, After myotube formation, synaptotagmin immunoreactivity begins to disappear from primary nerve branches but remains distributed within more distal branches. *I–L*, During the last 8 d of the pupal stage, the newly formed myotubes become striated, grow, and differentiate into adult muscle fibers. Synaptotagmin immunoreactivity becomes progressively restricted to terminal varicosities as the muscle fibers reach their final size. Scale bar, 10 μm.

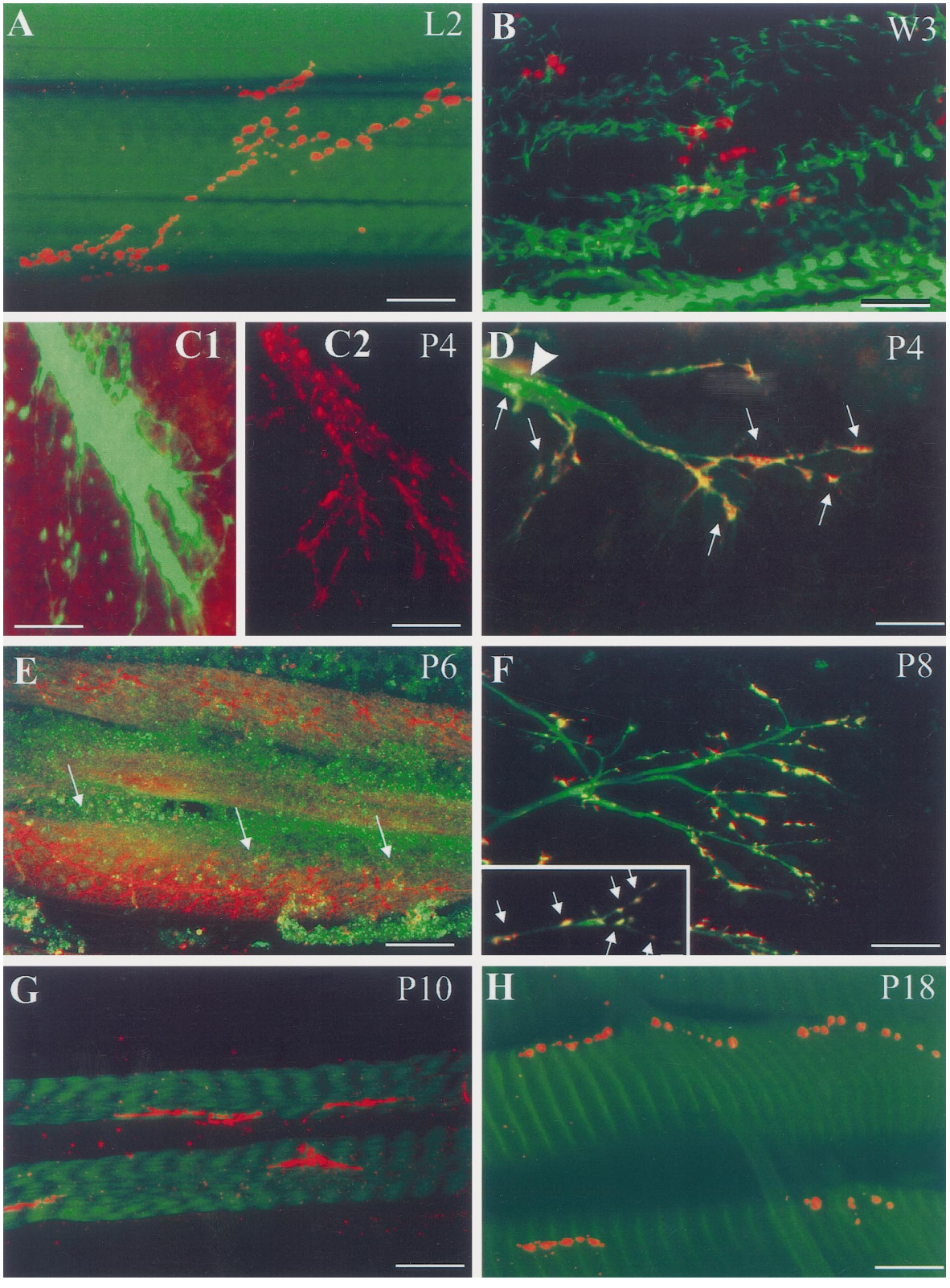

Figure 4. Relationship between presynaptic varicosities or nerve branches and the PrtFlx muscle or muscle anlage that they supply. Presynaptic varicosities or growing nerve branches were revealed with a polyclonal antibody against synaptotagmin (*red*), and the filamentous actin within muscles was labeled with Oregon Green phalloidin (*green*) in all but *C1, D*, and *F*. In *C1*, the motor endings were labeled with biocytin diffusion, and the staining was revealed with fluorescein-conjugated streptavidin (*green*), whereas the myonuclei were stained with propidium iodide (*red*). In panels *D* and *F* the nerve branches were filled with biocytin diffusion (*green*) and then processed for synaptotagmin immunostaining (*red* or *yellow*). *A, B*, Synaptotagmin immunoreactivity is localized in presynaptic varicosities over the intact (*A*) or degenerating (*B*) larval PrtFlx muscle. *C1, C2*, During the initial stages of adult PrtFlx muscle formation, enlarged motor branches grow over the anlage (*C1*). Synaptotagmin immunoreactivity is distributed widely in a punctate manner within the growing nerve branches (*C2*, same region from a different preparation). *D*. At a lower *(Figure legend continues)*

Labeling of filamentous actin and nuclei. To determine the presence of intact or differentiated muscles in whole mounts and sectioned preparations, filamentous actin within the muscles was labeled with BODIPY FL phallacidin or Oregon Green phalloidin (both from Molecular Probes). Whole-mount preparations were fixed in 4% paraformaldehyde in PBS for 4 hr to overnight. After washing with PBS and PBSX (1% Triton-100 in PBS) several times, nonspecific activity was blocked with 10% NGS in PBSX for 30 min, and then the preparations were incubated in 66 nM BODIPY FL phallacidin or Oregon Green phalloidin in PBS overnight in 4°C. In many cases, the nuclei of all classes of cells were revealed by incubating in 25 μM propidium iodide (Sigma) in PBS for 7 min (Sun et al., 1993) without pretreatment with RNase to eliminate the free distributed RNA in the cytoplasm of the cells. Therefore, in addition to the nucleus, the cytoplasm was lightly stained.

Confocal microscopy. The stained preparations were viewed with a confocal microscope (MRC-600 with a Nikon Optiphot-2 microscope and a krypton/argon laser light source; Bio-Rad). In cases in which two dyes were used, the images were merged by using different pseudocolors (red for Cy3-conjugated streptavidin or propidium iodide; green for streptavidin-dichlorotriazinyl amino fluorescein, Oregon Green phalloidin, FM1-43, or BODIPY FL phallacidin). Images were prepared using Confocal Assistant (Bio-Rad) and Corel Draw 6 (Corel) and printed on a Tektronix dye-sublimation printer.

RESULTS

Remodeling of the pretarsal flexor muscle during metamorphosis

General features of the remodeling of the *Manduca* leg neuromuscular system have been described previously (Consoulas et al., 1997). The present study focused on the pretarsal flexor muscle (PrtFlx) of the prothoracic legs to understand the relationship between presynaptic and postsynaptic differentiation. In the larva, this muscle has closely packed fibers bearing different sizes of nuclei (Fig. 1*A*). During the initial days of the last larval instar (L0–L3) the muscle was intact and responded to mechanical or electrical stimulation. PrtFlx muscle degeneration occurred between stages W0 and W3. At the same time, the unguitractor tendon, onto which the adult PrtFlx muscle will later attach, began to develop from an invagination of the epidermis near the tip of the imaginal (developing adult) leg. Muscle degeneration on day W0 was marked by the appearance of gaps between the fibers and, by stage W2, many large vacuoles in the cytoplasm and blistering of the sarcolemma (data not shown). By the end of stage W2, the cross-striations had disappeared, and within a few hours many of the larval myonuclei became apoptotic (Fig. 1*B*). After pupation, a homogeneous population of spindle-shaped cells (imaginal myoblasts; see Consoulas and Levine, 1997), originating mainly in coxa, migrated and became distributed within the leg segments (Fig. 1*C*). By the end of stage P2, myoblasts began to accumulate close to the unguitractor tendon in which the terminal processes of the PrtFlx motoneurons grew, became aligned at a 30° angle with the tendon, and fused (Fig. 1*D*; Consoulas et al., 1996; Consoulas and Levine, 1997). During subsequent pupal stages (P3–P8) the initial muscle anlage increased in size because of the continued accumulation and proliferation of myoblasts (Fig. 1*E,F*). Myotube formation began by stage P4, separation of myotubes from each other began by stage P6, and by stage P8 all of the fibers were clearly separate. Throughout the same period, free myoblasts continued to accumulate, proliferate, and fuse with the muscle fibers that had already formed (Fig. 1*G*). Myoblast proliferation declined by the time the fibers became striated (stage P9). During subsequent stages of adult development, the muscle fibers increased further in diameter and became well-separated from each other, with myonuclei distributed near the outer surface of the fibers (Fig. 1*H*).

Remodeling of PrtFlx muscle innervation during metamorphosis

The larval leg motoneurons persist during metamorphosis to innervate the new adult leg muscles (Kent and Levine, 1988). The peripheral processes of these persistent motoneurons first retract after the loss of their larval target muscles and then re-expand to innervate the adult muscles (Consoulas et al., 1996). The PrtFlx muscle is supplied by three persistent excitatory motoneurons (K. Oanh-Phan and U. Rose, personal communication). In both stages, individual fibers are either singly innervated by one fast motoneuron or dually innervated by one fast and one slow motoneuron, which were not distinguished in this study. To reveal the developmental fate of the motoneuron terminal axon branches, the main leg nerve 2a was filled with biocytin. In the larva, the motoneuron axons run through nerve 2a to supply the PrtFlx muscle fibers (Fig. 2*A*). During the early phase of PrtFlx muscle degeneration (stage W2), the high-order motor branches began to retract. After the breakdown of the muscle (stage W3) several secondary and high-order branches, as well as many terminal varicosities, disappeared, whereas the remaining branches occupied a central position within the femorotibial segment of the imaginal leg (Fig. 2*B*). By the end of the larval life (stage W4) the imaginal leg had grown considerably, and the retracted PrtFlx motor branches began to re-expand. During stage P2 the retracted nerve axons continued to expand over the inner surface of the imaginal epidermis in contact with accumulating imaginal myoblasts (Fig. 2*C*). By stage P3, the secondary and high-order nerve axons were expanding over the developing PrtFlx muscle anlage, as thin processes started to appear along these branches. Extensive nerve growth was apparent during the next days of pupal development (stages P5–P10; Fig. 2*D,E*). By stage P12 the innervation pattern had most of the features of the adult pattern, but distal nerve processes were still growing (Fig. 2*F*). The remaining stages of pupal development (P12–P18) were devoted to the establishment of adult terminal varicosities (see below).

In summary, the axons and terminal processes of the PrtFlx motoneurons undergo extensive remodeling after the larval muscle degeneration (stages W2–W4), characterized by a phase of axonal retraction and the loss of terminal varicosities, followed by a phase of axonal growth, during which myoblasts migrate and accumulate close to the terminal processes of the motoneurons (stages W4–P3). A third phase of rapid and extensive nerve growth over the developing PrtFlx muscle anlage follows (stages

←

magnification it is possible to see that punctate regions of synaptotagmin immunoreactivity are apparent in the primary axon (*arrowhead*), and in secondary and high-order distal branches and branch points (*arrows*). *E*, Early in stage P6, synaptotagmin immunoreactivity remains distributed in primary, secondary, and high-order nerve branches. *Arrows* indicate the PrtFlx muscle anlage. At this stage, large round hemocytes are stained with Oregon Green phalloidin (Consoulas et al., 1997). *F*, After the formation of muscle fibers, synaptotagmin immunoreactivity disappears from primary motor axon branches (data not shown) and becomes restricted to secondary and high-order branches and branch points. Aggregates of synaptotagmin immunoreactivity are apparent along high-order nerve processes (*arrows* in *inset*). *G, H*, After the muscle fibers become striated and during the later pupal stages, synaptotagmin immunoreactivity becomes progressively restricted to presynaptic varicosities. Note absence of staining in preterminal axon branches. Scale bars: *A, B, G, H*, 20 μm; *C1, C2*, 10 μm; *D*, 50 μm; *F*, 50 μm, *inset* in *F*, 10 μm; *E*, 200 μm.

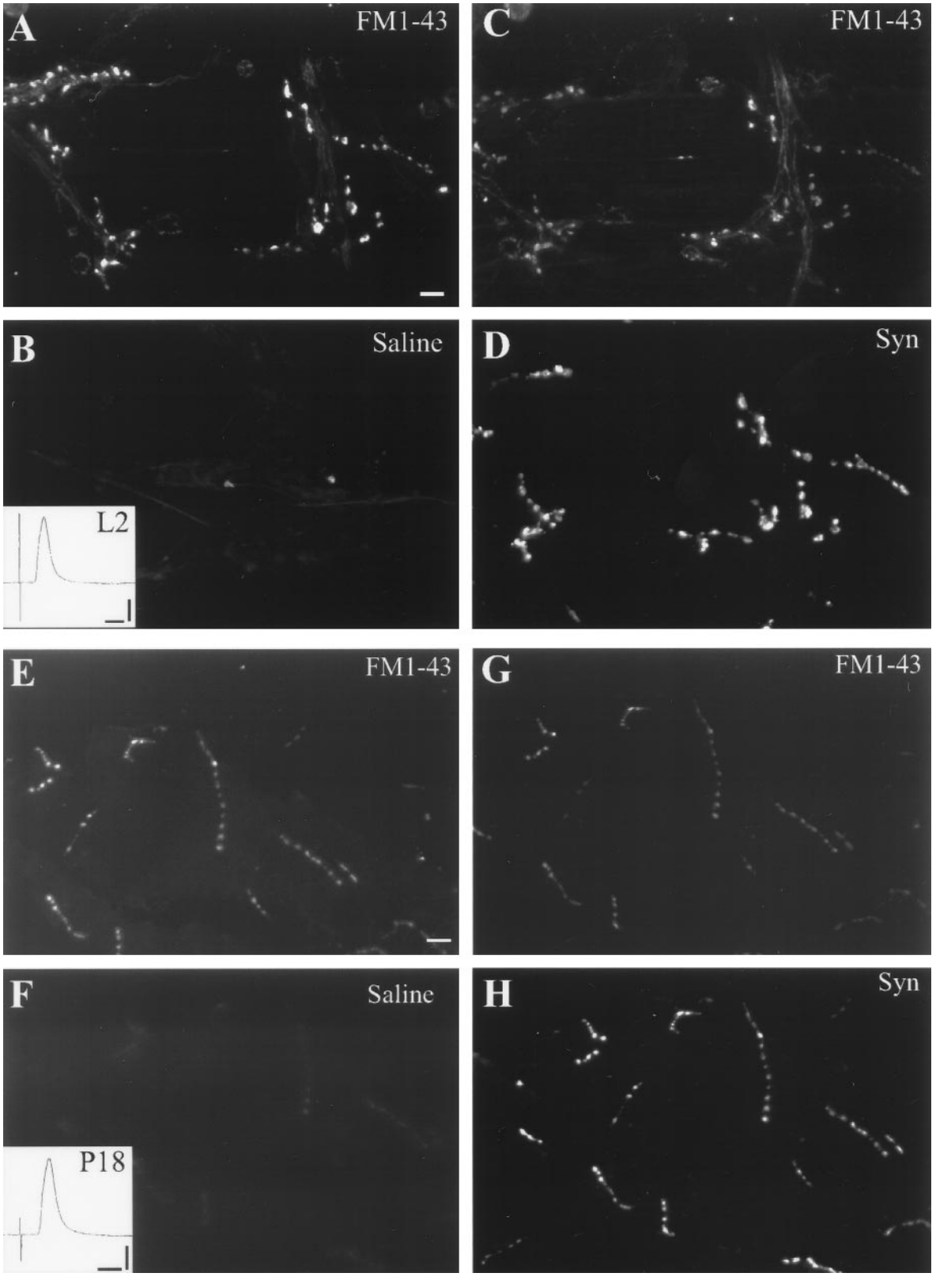

Figure 5. Activity-dependent synaptic vesicle recycling in motor terminals over the intact larval (*A–D*, stage L2) and adult (*E–H*, stage P18) PrtFlx muscle. Confocal micrographs were taken *in situ* from whole-mount preparations. Electrically stimulated presynaptic terminals became loaded when FM1-43 was applied in normal saline. The preparations were washed for 20 min in Ca^{2+}-free saline and viewed (*A, E*, *FM1-43*). The same motor terminals were then unloaded, by restimulating the nerve in the absence of FM1-43 in saline (*B, F*, *saline*), and then reloaded with FM1-43 (*C, G*, *FM1-43*). Finally, the preparations were fixed and processed for synaptotagmin immunolocalization (*D, H*, *Syn*). Note that the images in *A, C,* and *D* are almost identical, as are those in *E, G,* and *H*. *Insets* in *B* and *F* show the large EJPs recorded from the PrtFlx muscle fibers in response to nerve stimulation during the course of the experiments. Scale bar, 10 μm; calibration (*inset*): 10 mV, 10 msec.

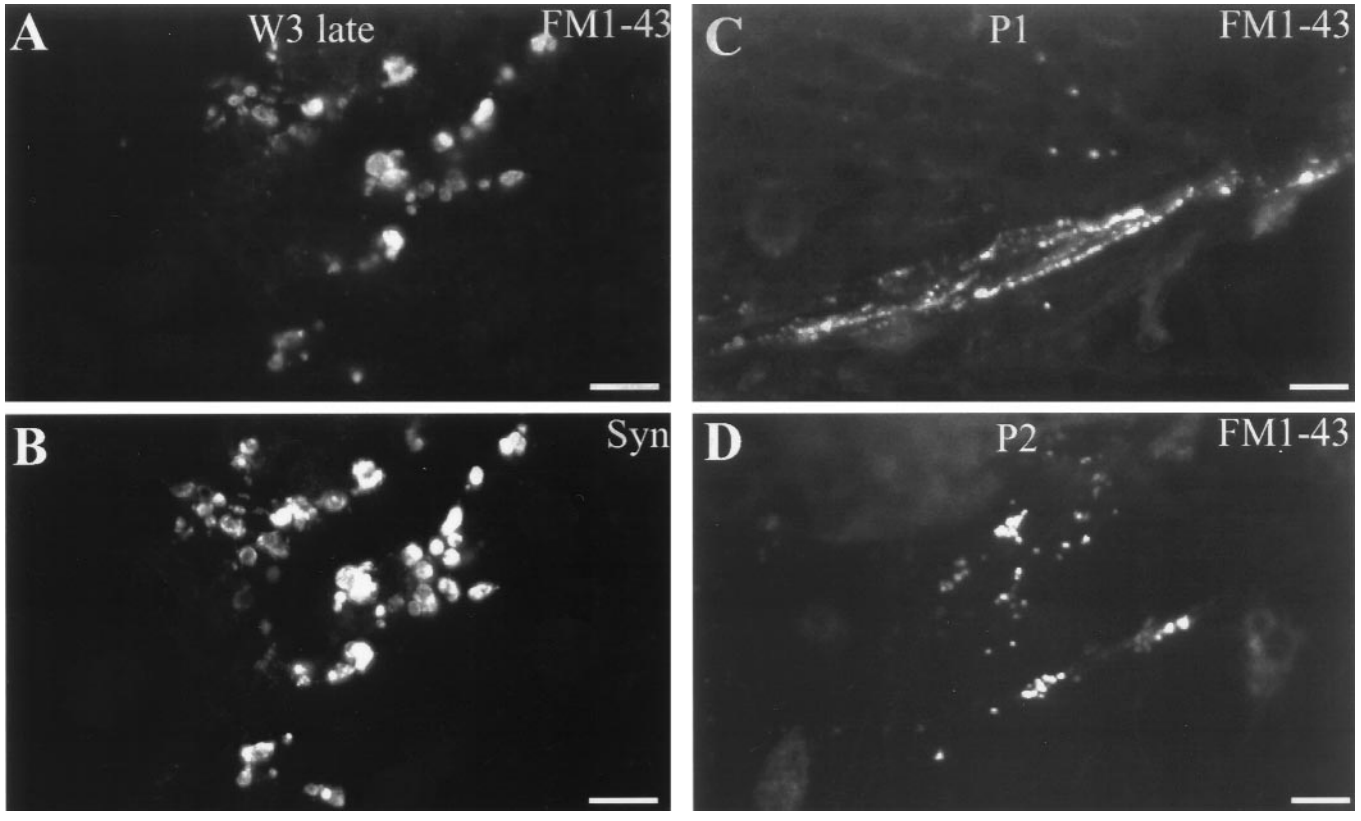

Figure 6. Activity-dependent synaptic vesicle recycling in motor terminals after the degeneration of the larval PrtFlx muscle. *A, B* (stage W3-late), Confocal micrographs taken *in situ* from the same whole-mount preparation. Presynaptic terminals were loaded by electrically stimulating nerve 2a in the presence of FM1-43 in normal saline. The neuromuscular preparation was washed for 30 min in Ca^{2+}-free saline and viewed (*A, FM1-43*). The terminals were then unloaded by restimulating the nerve in the absence of FM1-43 in saline (data not shown) and then reloaded (data not shown), and the preparation was fixed and processed for synaptotagmin immunolocalization (*B, Syn*). Note that the images in *A* and *B* are almost identical. *C, D*, Activity-dependent synaptic vesicle recycling in re-expanding PrtFlx motor terminals before muscle anlage formation (stages P1 and P2). Presynaptic terminals were loaded by electrically stimulating nerve 2a in the presence of FM1-43 in normal saline. The preparations were washed for 60 min in Ca^{2+}-free saline and viewed. Note that synaptic vesicle recycling occurs in punctate domains within the nerve branches. Scale bars, 10 μm.

P3–P12), with higher-order branch growth and maturation of the adult terminal varicosities marking the final phase.

Synaptotagmin immunolocalization

As an initial step in determining the fate of presynaptic specializations during the retraction and re-expansion of PrtFlx motoneuron terminals, the distribution of immunoreactivity for the synaptic vesicle membrane protein synaptotagmin was examined (Figs. 3, 4). During the first days of the last larval instar (stages L0–W2b-late), when the PrtFlx muscle is intact, synaptotagmin immunoreactivity was restricted to terminal varicosities (Figs. 3*A*, 4*A*). After muscle degeneration (stages W3 and W4), terminals became enlarged, reminiscent of the "retraction bulbs" seen in vertebrate muscles during synapse elimination (Riley, 1977). These enlarged nerve endings were immunopositive for synaptotagmin; there was no staining in the preterminal axons (Figs. 3*B,C*, 4*B*). During the early stages of pupal development (stages P0–P2-late), the retracted terminals began to lose their varicose appearance and were replaced by thin processes that grew in contact with the epidermis and migrating myoblasts. During this phase of nerve outgrowth, synaptotagmin immunoreactivity became widely distributed, not only within the high-order terminal processes, but also within the primary and secondary PrtFlx nerve branches and axons throughout the main leg nerve (Fig. 3*D,E*). Although widely distributed within these processes, the staining was punctate rather than uniform. Between stages P2-late and P6, thick primary and secondary branches with thin high-order terminal processes grew over the developing PrtFlx muscle anlage (Fig. *4C1*). Synaptotagmin immunoreactivity remained distributed in a punctate manner within all of these processes (Figs. 3*F,G*; 4*C2,D,E*). During stages P6–P8, synaptotagmin immunoreactivity disappeared from primary nerve branches but remained distributed in secondary and high-order branches, especially at branch points and in the thin terminal processes that grew over the surface of the myotubes (Figs. 3*H*, 4*F*, *arrows*). During subsequent stages of muscle development (stages P8–P18), synaptotagmin immunoreactivity became gradually restricted to high-order terminal branches over the developing muscle fibers and finally to terminal varicosities over the mature adult muscle fibers (Figs. 3*I–L*, 4*G,H*).

Synaptic vesicle recycling during the remodeling of PrtFlx muscle innervation

The styryl dye FM1-43, which allows the direct study of synaptic vesicle exocytosis and recycling (Betz and Bewick, 1992, Betz et al., 1992), was used to correlate the distribution of synaptotagmin immunoreactivity with the functional maturation of the neuromuscular transmission during muscle remodeling. Motoneurons

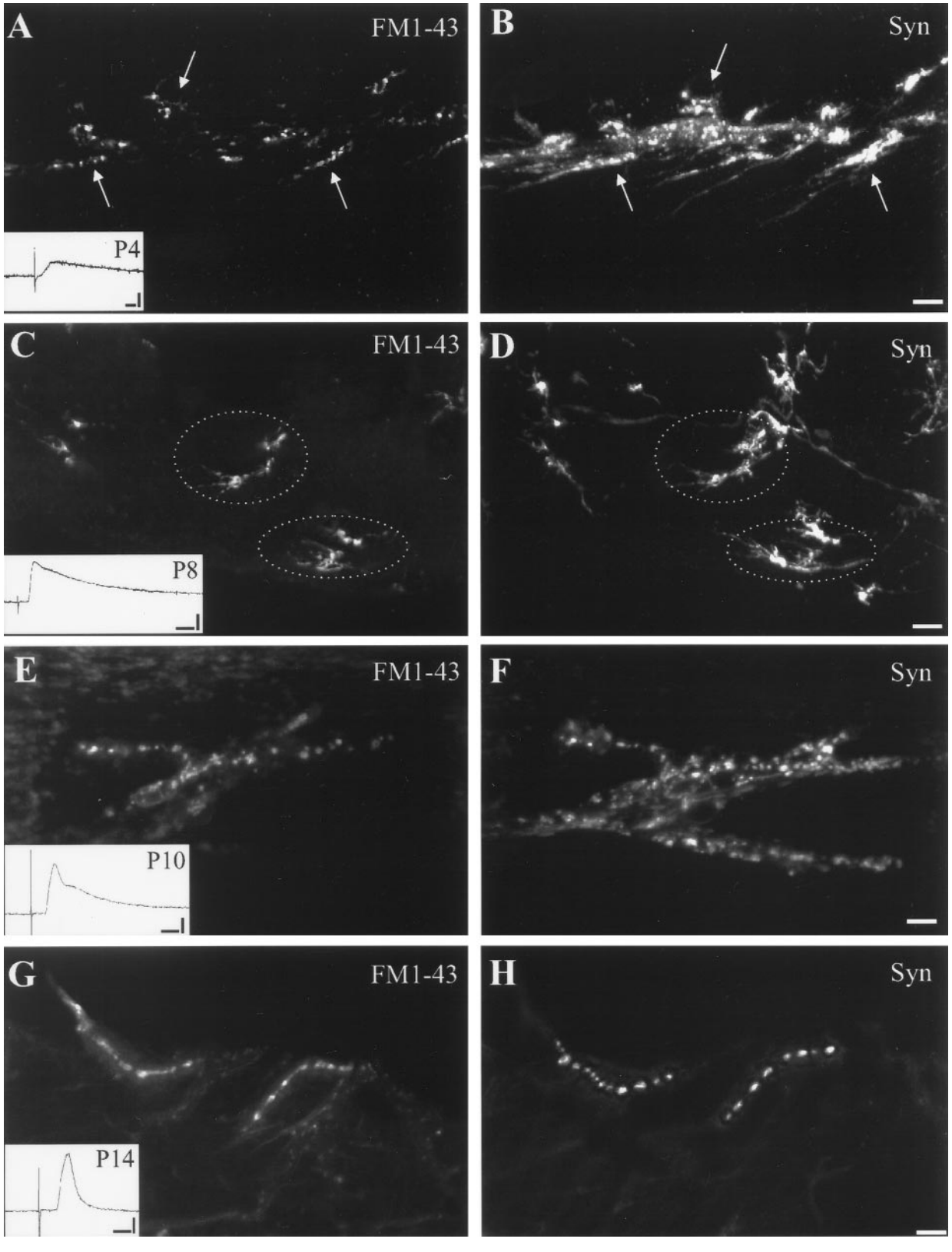

Figure 7. Activity-dependent synaptic vesicle recycling in motor terminals over the developing PrtFlx muscle. *A, B* (stage P4-late). Presynaptic terminals were loaded by electrically stimulating nerve 2a in the presence of FM1-43 in normal saline. The neuromuscular preparation was washed for 60 min in Ca^{2+}-free saline and viewed (*A, FM1-43*), and then the preparation was fixed and processed for synaptotagmin immunolocalization (*B, Syn*). Note that synaptic vesicle recycling occurs in domains localized in primary and secondary nerve branches, but synaptotagmin staining has a wider distribution throughout the nerve, including more distal processes (*arrows* indicate same areas in panels *A*, *B*). At this and stage P8 (*C, D*), stimulation-dependent unloading of FM1-43 was demonstrated in separate preparations (see Results). *C, D* (stage P8; same protocol as in *A, B*), Synaptic vesicle recycling occurs in domains that are localized in high-order branches and branching points, but synaptotagmin immunoreactivity is more *(Figure legend continues)*

in dissected leg preparations from different developmental stages were electrically stimulated in the presence of 4 μM FM1-43 in normal *Manduca* saline (4 mM Ca^{2+}). In unwashed preparations, the dye caused staining of all membranes. After washing the preparations in Ca^{2+}-free saline for 20–95 min, depending on the stage (Table 1), labeling remained only in the terminals of the stimulated PrtFlx motoneurons. Nonstimulated terminals over other muscles were devoid of staining after washing. No staining was observed in terminals that had been stimulated in the presence of FM1-43 in Ca^{2+}-free saline or in washed terminals after they had been exposed to FM1-43 but not stimulated (data not shown). Terminals could be loaded after they had been exposed to FM1-43 in high-K^+ saline (data not shown), but the staining was generally weaker than in terminals of motor axons that had been electrically stimulated. To ensure that FM1-43 labeled the presynaptic sites specifically, the following protocol was used for most of the developmental stages (L2, W4, P10, P14, and P18): (1) to load the PrtFlx motor terminals with the dye, nerve 2a (which contains the axons of PrtFlx motoneurons) was electrically stimulated in the presence of FM1-43 in normal saline; the preparation was then washed in Ca^{2+}-free saline, and confocal images were taken with the minimum possible exposure to fluorescent light; (2) to unload the terminals, the same preparation was restimulated in the absence of FM1-43 in normal saline, washed in Ca^{2+}-free saline, and imaged; (3) restimulation of the same terminals in the presence of FM1-43 in normal saline led to a second loading with the dye; and (4) after taking images from the reloaded terminals, the preparation was fixed and processed for anti-synaptotagmin immunostaining (Figs. 5, 6*A,B*, 7*E–H*). This protocol was modified, as described below, for experiments performed on stage P1–P8 animals (Figs. 6*C,D*, 7*A–D*; Table 1) because both the developing nerves and muscle fibers were fragile and degraded rapidly. Where possible, the postsynaptic responses to nerve stimulation were also monitored by recording intracellularly from muscle fibers to confirm functional synaptic transmission.

Images from motor terminals over the intact larval and adult PrtFlx muscle (stages L2 and P18) that were loaded with the FM1-43 were identical to those taken after synaptotagmin immunolocalization, thus confirming that these varicosities are sites of synaptic vesicle release (Fig. 5). Staining was restricted to terminal varicosities. Synaptic vesicle recycling was still apparent after the degeneration of the larval PrtFlx muscle and was restricted to the retracted motor terminal varicosities that were synaptotagmin-immunopositive (Fig. 6*A,B*; stage W3-late).

During myoblast production, migration, and accumulation at the site of the adult PrtFlx muscle formation (stages P0–P3), motor axons over the epidermis in the region where the PrtFlx anlage will form still became loaded with FM1-43 after nerve stimulation (Table 1, Fig. 6*C,D*; stages P1 and P2). In these early pupal stages the fragile nature of the preparations precluded our ability to demonstrate unloading of stained terminals or to fix and process FM1-43-loaded terminals for synaptotagmin immunoreactivity. However, no FM1-43 loading occurred when nerves were stimulated in Ca^{2+}-free saline or in nonstimulated terminals after exposure to FM1-43 and washing in normal saline.

During stages P4 and P8 the ability to load and unload terminals with FM1-43 was demonstrated in one set of experiments (data not shown), and in another set of experiments FM1-43-loaded terminals were imaged and then fixed and processed for anti-synaptotagmin staining (Fig. 7*A–D*). Activity-dependent FM1-43 loading could readily be demonstrated at late stage P4 (Fig. 7*A,B*), during which enlarged secondary branches of PrtFlx motoneurons grew over the muscle anlage (Fig. 4*C1,C2*). During this phase of development, as myoblasts continue to accumulate in the anlage, proliferate, and form myotubes, small excitatory junction potentials (EJPs) were successfully recorded in the central areas of the anlage, where the primary and secondary nerve branches were present, but were usually absent in the peripheral areas where high-order collaterals grew. The FM1-43-loaded presynaptic domains were localized to the primary and secondary axon branches and to a few high-order collaterals that were synaptotagmin-immunopositive (Fig. 7*A,B*). However, FM1-43 incorporation was absent from many regions of the nerve branches that were synaptotagmin-immunoreactive, including most of the high-order collaterals.

After myotube formation and separation was completed (stage P8), FM1-43 and synaptotagmin immunoreactivity disappeared from primary branches that were no longer in physical contact with the myotubes and became colocalized within secondary and high-order nerve branches that were growing along them (Fig. 7*C,D*; also see Fig. 4*F*). The strongest FM1-43 and synaptotagmin staining was found at branching points.

For the remaining stages, FM1-43 loading and unloading and synaptotagmin distribution could again be examined in the same motor terminals. After the muscle fibers became striated, punctate FM1-43 staining was revealed in high-order branches and branch points where synaptotagmin immunoreactivity was colocalized (Fig. 7*E,F*). During subsequent stages of neuromuscular development, areas of synaptic vesicle recycling were gradually restricted to terminal varicosities that were also synaptotagmin-immunopositive (Figs. 5*E–H*, 7*G,H*).

Based on findings of this and previous studies (Consoulas et al., 1996, 1997), neuromuscular remodeling during metamorphosis can be divided into the following sequence (Fig. 8):

(1) Stages L2–W0. Functional motor terminals on the intact PrtFlx muscle fibers comprise rosettes of varicosities in which synaptotagmin and FM1-43 staining are strictly co-localized.

(2) Stages W0–W4. During larval muscle degeneration some distal motor branches disappear, whereas the remaining retract to a central region within the imaginal leg. Despite the absence of a target muscle, synaptotagmin immunoreactivity and FM1-43 loading are colocalized within enlarged larval motor terminals that remain intact.

(3) Stages W4–P2-late. Imaginal myoblasts initially become distributed within the imaginal leg and then migrate and accu-

←

widely distributed (compare areas within *ellipses*). *E, F* (stage P10), Presynaptic terminals were loaded by electrically stimulating nerve 2a in the presence of FM1-43 in normal saline. The neuromuscular preparation was washed for 40 min in Ca^{2+}-free saline and viewed (*E, FM1-43*). The terminals were unloaded, by restimulating the nerve in the absence of FM1-43 in saline (data not shown), and then reloaded with FM1-43 (data not shown) and the preparation was fixed and processed for synaptotagmin immunolocalization (*F, Syn*). Note that FM1-43 and synaptotagmin staining reveal similar regions of punctate staining in high-order branches, but synaptotagmin immunoreactivity remains more widely distributed than sites of vesicular recycling. *G, H* (stage P14; same protocol as in *E, F*), Note that the FM1-43 and synaptotagmin images reveal similar regions of punctate staining within developing terminal branches of the motor axons. Scale bars, 10 μm. Calibration (*insets*): horizontal, 10 msec; vertical, *A*, 2 mV; *C, E*, 5 mV; *G*, 10 mV.

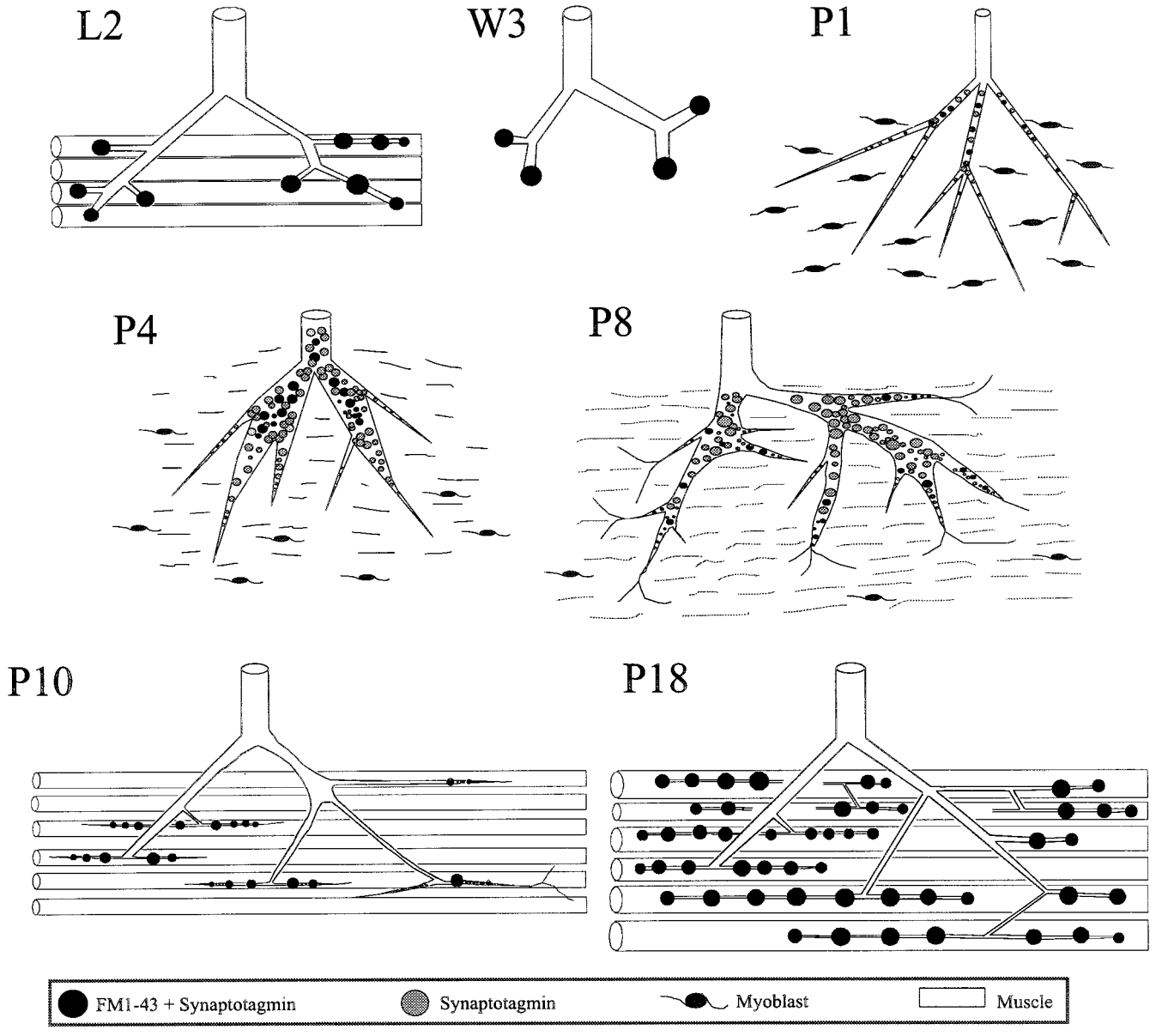

Figure 8. Summary of events of PrtFlx muscle presynaptic remodeling during metamorphosis (see Results). Synaptotagmin localization and active presynaptic sites viewed with FM1-43 are indicated.

mulate close to the nerve terminals to form the adult PrtFlx muscle anlage, over which motor branches begin to expand. Synaptotagmin immunoreactivity and FM1-43 loading are widely distributed in a punctate manner within nerve branches.

(4) Stages P2-late–P4. As myoblasts accumulate, proliferate, fuse, and differentiate into myotubes, synaptotagmin immunoreactivity remains distributed within axons and terminal processes. FM1-43 loading is detectable in more restricted axonal regions.

(5) Stages P4–P8. As myoblast proliferation declines and myotube separation is completed, synaptotagmin immunoreactivity begins to disappear gradually from proximal parts of the motor axons. Synaptic vesicle recycling, as indicated by FM1-43, becomes progressively localized to more distal branches.

(6) Stages P8–adult. Muscle fibers become striated but continue to grow until the end of pupation. Synaptotagmin and FM1-43 staining become tightly colocalized to terminal varicosities.

DISCUSSION

Persistence of motor terminals in the absence of muscle

Synaptotagmin immunoreactivity and sites of FM1-43 uptake and release remain colocalized within varicosities that persist after the breakdown of the larval muscle. These enlarged varicosities may represent a coalescence of many smaller terminals as the muscle fibers shrink and nerve branches retract. Enlargement of varicosities may involve some of the same mechanisms that are associated with the remodeling of motor terminals during synapse elimination and muscle growth in vertebrates (Balice-Gordon and Lichtman, 1990; Colman and Lichtman, 1993). In amphibians, target-deprived nerve terminals with intact basal lamina and associated glia can persist in synaptic sites for up to 1 year (Yao, 1988) and remain functional, in terms of vesicular release, for up to 5 months (Dunaevsky and Connor, 1995). Whether motor

terminal survival in *Manduca* is attributed to a muscle-derived factor that remains after the muscle death, as has been suggested for other preparations (Ko, 1984; Dunaevsky and Connor, 1995), remains to be investigated.

Presynaptic function during initial phases of adult muscle development

During the initial phase of adult muscle development (stages P0–P4; Fig. 8*C*), the axons of the persistent larval motoneurons undergo growth in association with imaginal myoblasts that form the adult PrtFlx muscle anlage. Indeed, nerve and muscle interactions are essential for the development of the adult muscles during insect metamorphosis (Nüesch, 1985; Currie and Bate, 1995; Hegstrom and Truman, 1996; Bayline et al., 1998). In the developing adult legs of *Manduca*, both the accumulation of myoblasts into the correct sites of muscle formation and the appropriate level of proliferation are dependent on innervation (Luedeman and Levine, 1996; Consoulas and Levine, 1997).

Despite the lack of a functional target during early stages of adult development, Ca^{2+}-dependent synaptic vesicle exocytosis is maintained. Functional contact with the new target could be demonstrated as soon as initial myotubes formed. Synaptotagmin is distributed along the axons of the motoneurons, suggesting that synaptic vesicles or their precursors are relocalized or being transported, as reported in mammals and *Drosophila* during embryogenesis (Kelly and Zacks, 1969; Kullberg et al., 1977; Lupa and Hall, 1989; Littleton et al., 1993; Yoshihara et al., 1997) or for neurons isolated *in vitro* (Matteoli et al., 1992; Kraszewski et al., 1995). Synaptic vesicle exocytosis and recycling, however, requires the presence of well-orchestrated action of several synaptic vesicle and plasma membrane proteins, in addition to synaptotagmin (Südhof, 1995). The ability of persistent axon branches to undergo FM1-43 loading suggests that a degree of functional specialization of the presynaptic machinery is maintained.

During embryonic development, neuronal growth cones are capable of neurotransmitter release before contact with the target (Hume et al., 1983; Young and Poo, 1983; Chow and Poo, 1985; Xie and Poo, 1986; Sun and Poo, 1987). Functional synaptic transmission can be detected shortly after the initial neuronal growth cone and myotube contact (Bennett and Pettigrew, 1974; Blackshaw and Warner, 1976; Kullberg et al., 1977; Dennis, 1981; Kidokoro and Yeh, 1982; Broadie and Bate, 1993a). This contact between the nerve and muscle cell membranes triggers an increase in neurotransmitter release that is driven by a rise in resting presynaptic Ca^{2+} concentration (Chow and Poo, 1985; Xie and Poo, 1986; Funte and Haydon, 1993; Zoran et al., 1993). Retrograde signal(s) from the target may be responsible (Connor and Smith, 1994). Similarly, in the present study, the maintenance of presynaptic function after muscle degeneration may reflect an autonomous ability of the persistent motor axons to express presynaptic specializations, or persistent cues from the larval target, combined with additional signals from the muscle precursors and the steroid hormone environment (see below).

Progressive restriction of synaptic vesicles and presynaptic function to mature synapses

During later stages of muscle development, before the establishment of final synaptic sites, synaptotagmin is distributed first within axons and then progressively to more distal processes. Calcium-dependent vesicle exocytosis and recycling is more restricted and first occurs in the shafts of motor axons rather than the higher-order branches that will later give rise to the mature presynaptic varicosities. These data are consistent with other observations that the machinery for vesicular cycling is present in developing axons before the formation of mature synapses. In cultured hippocampal neurons, for example, both Ca^{2+}-dependent glutamate release and clustering and exocytosis of vesicles occur in the axon shafts of immature neurons before establishment of any synaptic contact (Kraszewski et al., 1995; Verderio et al., 1995). Similarly, in the *Drosophila* embryo, the initial formation of active zones can occur within motor axons in the absence of muscles (Prokop et al., 1996). This appearance of presynaptic specializations before the establishment of final synaptic sites may be analogous to the unlocalized distribution of glutamate or acetylcholine receptors on muscles before innervation (Broadie and Bate, 1993a,b; Hall and Sanes, 1993). Although both presynaptic and postsynaptic proteins may be expressed autonomously, the precise register of mature synaptic specializations probably requires cellular interactions in both directions (Prokop et al., 1996).

The differentiation of myotubes is an ongoing process; at any point in time different parts of the muscle anlage are in different states of development (Consoulas et al., 1997; this study). Initial presynaptic active sites in the axon shaft are transient and are gradually replaced by new sites in more distal processes as the muscle anlage grows and myotubes are formed. The correlation between the shifting location of functional sites of synaptic vesicle turnover and the progression of muscle differentiation within the enlarging anlage may reflect a retrograde cue that must be derived from myotubes once they reach the appropriate stage of development. The gradual shifting of presynaptic sites on maturing muscles represents an interesting contrast to embryonic neuromuscular junction formation in *Drosophila*, in which the neuronal growth cone stops as it reaches preformed myotubes and becomes transformed into a presynaptic terminal (Yoshihara et al., 1997).

Although the adult axonal branching pattern of the PrtFlx motoneurons has been established by stage P8, there is turnover of high-order branches, and the formation of new synaptic sites is continuous as muscle fibers elongate. A similar presynaptic remodeling has been observed during metamorphosis in amphibians. Postmetamorphic myogenesis and muscle fiber growth in frogs is accompanied by differential retraction, enlargement, creation, and elimination of junctional branches and synaptic sites (Sperry and Grobstein, 1983; Wernig and Herrera, 1986; Herrera and Werle, 1990; Herrera et al., 1990, 1991). Addition of new branches and synaptic sites has also been observed during the growth of body wall muscles in *Drosophila* (Budnik et al., 1990; Gorczyca et al., 1993; Keshishian et al., 1993, 1996).

Control of motor terminal remodeling

The central dendrites and the peripheral processes of the persistent motoneurons undergo simultaneous phases of regression and re-expansion (Kent and Levine, 1993; Consoulas et al., 1996). Although the fine details and terminal stages of dendritic growth and the differentiation of motor terminals may be regulated by cellular interactions (Kent and Levine, 1993; Truman and Reiss, 1995), many aspects of this remodeling are under the control of the steroid hormone 20-hydroxyecdysone (Weeks, 1987; Truman and Reiss, 1988; Weeks and Ernst-Utzschneider, 1989; Prugh et al., 1992; Truman and Reiss, 1995). Thus, ecdysteroids may act directly on the cell body of motoneurons (Levine et al., 1986; Levine, 1989; Prugh et al., 1992) to regulate the synthesis of proteins involved in the formation and maintenance of presynap-

tic machinery. It is likely, however, that the precise alignment of presynaptic and postsynaptic specializations requires communication between neuron and muscle. This can readily be addressed through manipulations of the muscle precursor cells both *in vivo* (Consoulas and Levine, 1997) and in nerve and muscle cocultures (Luedeman and Levine, 1996).

REFERENCES

Balice-Gordon RJ, Lichtman JW (1990) *In vivo* visualization of the growth of presynaptic and postsynaptic elements of mouse neuromuscular junctions. J Neurosci 10:894–908.

Bayline RJ, Khoo AB, Booker R (1998) Innervation regulates the metamorphic fates of larval abdominal muscles in the moth, *Manduca sexta*. Dev Genes Evol, in press.

Bell RA, Joachim FA (1976) Techniques for rearing laboratory colonies of tobacco hornworms and pink bollworms. Ann Entomol Soc Am 69:365–373.

Bennett MR, Pettigrew AG (1974) The formation of synapses in striated muscle during development. J Physiol (Lond) 241:515–545.

Betz WJ, Bewick GS (1992) Optical analysis of synaptic vesicle recycling at the frog neuromuscular junction. Science 255:200–203.

Betz WJ, Mao F, Bewick GS (1992) Activity-dependent fluorescent staining and destaining of living vertebrate motor terminals. J Neurosci 12:363–375.

Blackshaw S, Warner A (1976) Onset of acetylcholine sensitivity and endplate activity in developing myotome muscles of *Xenopus*. Nature 262:217–218.

Broadie KS, Bate M (1993a) Development of the embryonic neuromuscular synapse of *Drosophila melanogaster*. J Neurosci 13:144–166.

Broadie KS, Bate M (1993b) Innervation directs receptor synthesis and localization in *Drosophila* embryo synaptogenesis. Nature 361:350–353.

Budnik V, Zhong Y, Wu C (1990) Morphological plasticity of motor axons in *Drosophila* mutants with altered excitability. J Neurosci 10:3754–3768.

Chow I, Poo MM (1985) Release of acetylcholine upon contact with muscle cell. J Neurosci 5:1076–1082.

Colman H, Lichtman JW (1993) Interactions between nerve and muscle: synapse elimination at the developing neuromuscular junction. Dev Biol 156:1–10.

Connor EA, Smith MA (1994) Retrograde signaling in the formation and maintenance of the neuromuscular junction. J Neurobiol 25:722–739.

Consoulas C, Levine RB (1997) Accumulation and proliferation of adult leg muscle precursors in *Manduca* are dependent on innervation. J Neurobiol 32:531–553.

Consoulas C, Kent KS, Levine RB (1996) Remodeling of the peripheral processes and presynaptic terminals of leg motoneurons during metamorphosis of the hawkmoth, *Manduca sexta*. J Comp Neurol 372:415–434.

Consoulas C, Anezaki M, Levine RB (1997) Development of adult thoracic leg muscles during metamorphosis of the hawkmoth *Manduca sexta*. Cell Tissue Res 287:393–412.

Currie DA, Bate M (1995) Innervation is essential for the development and differentiation of a sex-specific muscle in *Drosophila melanogaster*. Development 121:2549–2557.

Dennis MJ (1981) Development of the neuromuscular junction: inductive interactions between cells. Annu Rev Neurosci 4:43–68.

Dubuque SH, Nighorn A, Gibson JH, Tolbert LP (1997) Tyrosine phosphorylation and synapse formation in developing olfactory glomeruli. Soc Neurosci Abstr 23:1975.

Dunaevsky A, Connor EA (1995) Long-term maintenance of presynaptic function in the absence of target muscle fibers. J Neurosci 15:6137–6144.

Funte LR, Haydon PG (1993) Synaptic target contact enhances presynaptic calcium influx by activating cAMP-dependent protein kinase during synaptogenesis. Neuron 10:1069–1078.

Gorczyca M, Augart C, Budnik V (1993) Insulin-like receptor and insulin-like peptide are localized at neuromuscular junctions in *Drosophila*. J Neurosci 13:3692–3704.

Hall ZW, Sanes JR (1993) Synaptic structure and development: the neuromuscular junction. Neuron 10:99–122.

Hegstrom CD, Truman JW (1996) Steroid control of muscle remodeling during metamorphosis in *Manduca sexta*. J Neurobiol 29:535–550.

Herrera AA, Werle MJ (1990) Mechanisms of elimination, remodeling, and competition at frog neuromuscular junctions. J Neurobiol 21:71:98.

Herrera AA, Banner LR, Nagaya N (1990) Repeated, *in vivo* observation of frog neuromuscular junctions: remodeling involves concurrent growth and retraction. J Neurocytol 19:85–99.

Herrera AA, Banner LR, Werle MJ, Regnier M, Nagaya-Stevens N (1991) Postmetamorphic development of neuromuscular junctions and muscle fibers in the frog *Cutaneous pectoris*. J Neurobiol 22:15–28.

Horikawa K, Armstrong WF (1988) A versatile means of intracellular labeling: injection of biocytin and its detection with avidin conjugates. J Neurosci Methods 25:1–12.

Hume RI, Role LW, Fischbach GD (1983) Acetylcholine release from growth cones detected with patches of acetylcholine receptor-rich membranes. Nature 305:632–634.

Kelly AM, Zacks SI (1969) The fine structure of motor endplate morphogenesis. J Cell Biol 42:154–169.

Kent KS, Levine RB (1988) Neural control of leg movements in a metamorphic insect: persistence of larval leg motor neurons to innervate the adult legs of *Manduca sexta*. J Comp Neurol 276:30–43.

Kent KS, Levine RB (1993) Dendritic reorganization of an identified neuron during metamorphosis of the moth *Manduca sexta*: the influence of interactions with the periphery. J Neurobiol 24:1–22.

Kent KS, Consoulas C, Duncan C, Johnston RM, Luedeman R, Levine RB (1995) Remodeling of neuromuscular systems during insect metamorphosis. Am Zool 35:578–584.

Keshishian H, Chiba A, Chang T, Halfton M, Harkins E, Jarecki J, Wang L, Anderson M, Cash S, Halpern M, Johansen J (1993) Cellular mechanisms governing synaptic development in *Drosophila melanogaster*. J Neurobiol 24:757–787.

Keshishian H, Broadie K, Chiba A, Bate M (1996) The *Drosophila* neuromuscular junction: a model for studying synaptic development and function. Annu Rev Neurosci 19:545–575.

Kidokoro Y, Yeh E (1982) Initial synaptic transmission at the growth cone in *Xenopus* nerve-muscle cultures. Proc Natl Acad Sci USA 79:6727–6731.

Ko CP (1984) Regeneration of the active zone at the frog neuromuscular junction. J Cell Biol 98:1685–1695.

Kraszewski K, Mundigl O, Daniel L, Verderio C, Matteoli M, De Camilli P (1995) Synaptic vesicle dynamics in living cultured hippocampal neurons visualized with CY3-conjugated antibodies directed against the lumenal domain of synaptotagmin. J Neurosci 15:4328–4342.

Kullberg RW, Lentz TL, Cohen MW (1977) Development of the myotomal neuromuscular junction in *Xenopus laevis*: an electrophysiological and fine structure study. Dev Biol 60:101–129.

Levine RB (1989) Expansion of the central arborizations of persistent sensory neurons during insect metamorphosis: the role of the steroid hormone, 20-Hydroxyecdysone. J Neurosci 9:1045–1054.

Levine RB, Truman D, Linn D, Bate CM (1986) Endocrine regulation of the form and function of axonal arbors during insect metamorphosis. J Neurosci 6:293–299.

Littleton JT, Bellen HJ, Perin MS (1993) Expression of synaptotagmin in *Drosophila* reveals transport and localization of synaptic vesicles to the synapse. Development 118:1077–1088.

Luedeman R, Levine RB (1996) Neurons and ecdysteroids promote the proliferation of myogenic cells cultured from the developing adult legs of *Manduca sexta*. Dev Biol 173:51–68.

Lupa MT, Hall ZW (1989) Progressive restriction of synaptic vesicle protein to the nerve terminal during development of the neuromuscular junction. J Neurosci 9:3937–3945.

Matteoli M, Takei K, Perin MS, Südhof TC, De Camilli P (1992) exoendocytotic recycling of synaptic vesicles in developing processes of cultured hippocampal neurons. J Cell Biol 117:849–861.

Nijhout HF, Williams CM (1974) Control of moulting and metamorphosis in the tobacco hornworm, *Manduca sexta* (L): growth of the last-instar larva and the decision to pupate. J Exp Biol 61:481–491.

Noakes PG, Gautam M, Mudd J, Sanes JR, Merlie JP (1995) Aberrant differentiation of neuromuscular junctions in mice lacking s-laminin/laminin $\beta 2$. Nature 374:258–262.

Nüesch H (1985) Control of muscle development. In: Comparative insect physiology, biochemistry, and pharmacology, Vol 2 (Kerkut GA, Gilbert LI, eds), pp 425–252. Oxford: Pergamon.

Perin MS, Fried VA, Mignery GA, Südhof TC, Jahn R (1990) Phospholipid binding by a synaptic vesicle protein homologous to the regulatory domain of protein kinase C. Nature 345:260–263.

Prokop A, Landgraf M, Rushton E, Broadie K, Bate M (1996) Presynaptic development at the *Drosophila* neuromuscular junction: assembly and localization of presynaptic active zones. Neuron 17:617–626.

Prugh J, Della Crose K, Levine RB (1992) Effects of the steroid hormone, 20-Hydroxyecdysone, on the growth of neurites by identified insect motoneurons *in vitro*. Dev Biol 154:331–347.

Ramaswami M, Krishnan KS, Kelly RB (1994) Intermediates in synaptic vesicle cycling revealed by optical imaging of *Drosophila* neuromuscular junctions. Neuron 13:363–375.

Reinecke JP, Buckner JS, Grugel SR (1980) Life cycle of laboratory-reared tobacco hornworms, *Manduca sexta*, a study of development and behavior using time-lapse cinematography. Biol Bull 158:129–140.

Riley DA (1977) Spontaneous elimination of nerve terminals from the endplates of developing skeletal myofibers. Brain Res 134:279–285.

Sanes JR, Marshall LM, McMahan UJ (1978) Reinnervation of muscle fiber basal lamina after removal of myofibers: differentiation of regenerating axons at original synaptic sites. J Cell Biol 78:176–198.

Sperry DG, Grobstein P (1983) Postmetamorphic changes in the lumbar lateral motor column in relation to muscle growth in the toad, *Bufo americanus*. J Comp Neurol 216:104–114.

Südhof TC (1995) The synaptic vesicle cycle: a cascade of protein-protein interactions. Nature 375:645–653.

Sun XJ, Tolbert LP, Hildebrand JG (1993) Ramification pattern and ultrastructural characteristics of the serotonin-immunoreactive neuron in the antennal lobe of the moth *Manduca sexta*: a laser scanning confocal and electron microscopic study. J Comp Neurol 338:5–16.

Sun YA, Poo MM (1987) Evoked release of acetylcholine from the growing embryonic neuron. Proc Natl Acad Sci USA 84:2540–2544.

Tolbert LP, Matsumoto SG, Hildebrand JG (1983) Development of synapses in the antennal lobes of the moth *Manduca sexta* during metamorphosis. J Neurosci 3:1158–1175.

Trimmer BA, Weeks JC (1989) Effects of nicotinic and muscarinic agents on an identified motoneurone and its direct afferent inputs in larval Manduca sexta. J Exp Biol 144:303–337.

Truman JW, Reiss SE (1988) Hormonal regulation of the shape of identified motoneurons in the moth, *Manduca sexta*. J Neurosci 8:765–775.

Truman JW, Reiss SE (1995) Neuromuscular metamorphosis in the moth *Manduca sexta*: hormonal regulation of synapse loss and remodeling. J Neurosci 15:4815–4826.

Verderio C, Coco S, Fumagali G, Matteoli M (1995) Calcium-dependent glutamate release during neuronal development and synaptogenesis: different involvement of ω-AgaIV A and ω-CTx-GVIA sensitive channels. Proc Natl Acad Sci USA 92:6449–6453.

Weeks JC (1987) Time course of hormonal independence for developmental events in neurons and other cell types during insect metamorphosis. Dev Biol 124:163–176.

Weeks JC, Ernst-Utzschneider (1989) Respicification of larval proleg motoneurons during metamorphosis of the tobacco hornworm, *Manduca sexta*: segmental dependence and hormonal regulation. J Neurobiol 20:569–592.

Wernig A, Herrera AA (1986) Sprouting and remodelling at the neuromuscular junction. Prog Neurobiol 27:251–291.

Xie ZP, Poo MM (1986) Initial events in the formation of neuromuscular synapse: rapid induction of acetlcholine release. Proc Natl Acad Sci USA 83:7069–7073.

Yao YM (1988) Maintenance of axon terminals at synaptic sites in the absence of muscle fibers. In: Current issues in neural regeneration research. (Reiet PJ, Bunge RP, Seil FJ, eds), pp 167–178. New York: Liss.

Yoshihara M, Rheuben MB, Kidokoro Y (1997) Transition from growth cone to functional motor nerve terminal in *Drosophila* embryos. J Neurosci 17:8408–8426.

Young SH, Poo MM (1983) Spontaneous release of transmitter from growth cones of embryonic neurons. Nature 305:634–637.

Zoran MJ, Funte LR, Kater SB, Haydon PG (1993) Contact with a synaptic target causes an elevation in a presynaptic neuron's resting calcium set-point. Dev Biol 158:163–171.